UNCL/
SECURI

AD-A209 623

DOCUMENTATION PAGE

1a. RE
UI

1b. RESTRICTIVE MARKINGS

2a. SE

3. DISTRIBUTION/AVAILABILITY OF REPORT

Approved for public release; distribution is unlimited.

2b. DECLASSIFICATION/DOWNGRADING SCHEDULE

4. PERFORMING ORGANIZATION REPORT NUMBER(S)

5. MONITORING ORGANIZATION REPORT NUMBER(S)

6a. NAME OF PERFORMING ORGANIZATION	6b. OFFICE SYMBOL (If applicable)	7a. NAME OF MONITORING ORGANIZATION
Naval Ocean Systems Center	NOSC	

6c. ADDRESS (City, State and ZIP Code)	7b. ADDRESS (City, State and ZIP Code)
San Diego, California 92152-5000	

8a. NAME OF FUNDING/SPONSORING ORGANIZATION	8b. OFFICE SYMBOL (If applicable)	9. PROCUREMENT INSTRUMENT IDENTIFICATION NUMBER
Defense Advance Research Projects Agency	DARPA	

8c. ADDRESS (City, State and ZIP Code)	10. SOURCE OF FUNDING NUMBERS			
	PROGRAM ELEMENT NO.	PROJECT NO.	TASK NO.	AGENCY ACCESSION NO.
1400 Wilson Blvd. Arlington, VA 22209	0602301E	EE87		DN388 650

DTIC
ELECTE
JUN 23 1989
S E D

11. TITLE (Include Security Classification)

CROSSTALK BETWEEN TWO COPLANAR WAVEGUIDES

12. PERSONAL AUTHOR(S)

G. A. Garcia, C. T. Chang

13a. TYPE OF REPORT	13b. TIME COVERED	14. DATE OF REPORT (Year, Month, Day)	15. PAGE COUNT
professional paper	FROM TO	June 1989	

16. SUPPLEMENTARY NOTATION

17. COSATI CODES			18. SUBJECT TERMS (Continue on reverse if necessary and identify by block number)
FIELD	GROUP	SUB-GROUP	GAAS silicon optics integration

19. ABSTRACT (Continue on reverse if necessary and identify by block number)

Mapping of two coplanar waveguides into parallel plate transmission lines is performed using elliptical integral transformations. This mapping provides more physical insight in estimation of capacitive crosstalk between two coplanar waveguides. Predictions of crosstalk levels agree reasonably well with the experimental measurements on the up-scaled coplanar waveguides with various separations. Scaling of coplanar waveguides does not change the characteristic impedance and the coupling capacitance per unit length. However, the total coupling capacitance varies linearly with scaling.

89 6 27 036

Published in *Kurzberichte - Letters*, AEU, Band 43 (1989) Heft 1.

20. DISTRIBUTION/AVAILABILITY OF ABSTRACT	21. ABSTRACT SECURITY CLASSIFICATION
☒ UNCLASSIFIED/UNLIMITED ☐ SAME AS RPT ☐ DTIC USERS	UNCLASSIFIED

22a. NAME OF RESPONSIBLE INDIVIDUAL	22b. TELEPHONE (Include Area Code)	22c. OFFICE SYMBOL
G. A. Garcia	(619) 553-3912	Code 553

DD FORM 1473, 84 JAN

83 APR EDITION MAY BE USED UNTIL EXHAUSTED
ALL OTHER EDITIONS ARE OBSOLETE

UNCLASSIFIED
SECURITY CLASSIFICATION OF THIS PAGE

Crosstalk Between Two Coplanar Waveguides

Mapping of two coplanar waveguides into parallel plate transmission lines is performed using elliptical integral transformations. This mapping provides more physical insight in estimation of capacitive crosstalk between two coplanar waveguides. Predictions of crosstalk levels agree reasonably well with the experimental measurements on the up-scaled coplanar waveguides with various separations. Scaling of coplanar waveguides does not change the characteristic impedance and the coupling capacitance per unit length. However, the total coupling capacitance varies linearly with scaling.

Übersprechen zwischen zwei planparallelen Wellenleitern

Die Abbildung von zwei planparallelen Wellenleitern auf parallele Streifenleitungen erfolgt mit elliptischen Integralen als Transformationsfunktionen. Dies ermöglicht eine bessere Beurteilung des kapazitiven Übersprechens. Die ermittelten Übersprechpegel stimmen relativ gut mit experimentellen Meßergebnissen an im vergrößerten Maßstab hergestellten planparallelen Wellenleitern mit verschieden weiten Abständen überein. Die Skalierung planparalleler Wellenleiter hat keinen Einfluß auf den Wellenwiderstand und den Koppelkapazitätsbelag. Der Wert der Koppelkapazität selbst ist proportional zum Skalierungsfaktor.

1. Introduction

Microstrip lines and coplanar waveguides (CPW) are the primary interconnect structures for monolithic microwave circuits and very high speed integrated circuits [1]. In comparing these transmission lines, the CPW offers some advantages over the microstrip line including easier connection to shunt circuit elements and maintenance of constant characteristic impedance when lateral dimensions are scaled. These advantages come about because the signal line and ground plane conductors of the CPW are located on the same side of the insulating substrate.

A price may have to be paid for this convenience, however, since the electric fields associated with the CPW are not as well confined to the immediate vicinity of the transmission line as is the case with the microstrip line. Because of the extended nature of the fields in the CPW, more care may be required in the design of dense circuitry that uses the CPW for interconnection if appreciable crosstalk between closely spaced lines is to be avoided. We present here a calculation of the crosstalk between two CPWs based on a quasi-static TEM approximation using an elliptical integral transformation. Predictions of crosstalk levels are in good agreement with experimental measurements on two CPWs with various separations.

2. Mapping of Two Coplanar Waveguides into Parallel Plate Transmission Lines

The cross-section of two CPWs is shown in Fig. 1. Here $2a$ is the signal conductor width, $2b$ is the separation between the ground conductors of a given CPW, $2c$ is the separation between centers of two signal conductors, and $(c' - b)$ is the fixed width of the other half CPW ground conductor. The second CPW signal conductor is located at $(2c - a) \leqq x \leqq (2c + a)$. To calculate the capacitive coupling between two CPWs, an elliptical integral transformation similar to that used by Wen [2] is used to convert the planar geometry of the CPW to the geometry of a parallel plate transmission line. This mapping provides more physical insight than the original planar geometry and allows the capacitive coupling to be readily approxi-

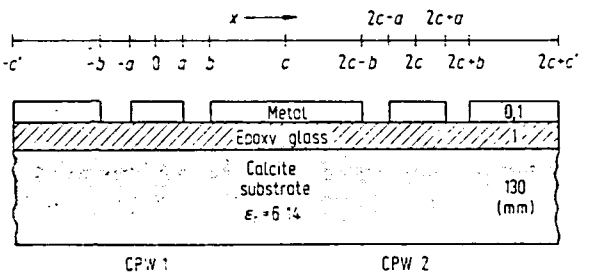

Fig. 1. Cross-section of two coplanar waveguides with signal conductor width $2a = 6$ mm, ground conductor separation for a given CPW $2b = 12$ mm, separation between two signal conductors $2c$ varying from 5 cm to 30 cm and outer ground conductor width $(c' - b) = 15$ cm.

mated. The elliptical integral transformation used here is defined by

$$z(x) = \int_0^x \frac{b\,dx}{\sqrt{(a^2 - x^2)(b^2 - x^2)}}. \tag{1}$$

The transformation can be expressed in terms of the general elliptical integral [3] as

$$F(\alpha, \phi) = \int_0^{\phi} \frac{d\theta}{\sqrt{1 - \sin^2 \alpha \sin^2 \theta}}, \tag{2}$$

where the angle α for our application is defined as

$$\alpha = \arcsin(a/b). \tag{3}$$

The relationships between x and θ in eqs. (1) and (2) are $x = a \sin\theta$, $x = b^2 - (b^2 - a^2)\sin^2\theta$, and $x = b/\sin\theta$ for $|x| \leqq a$, $a \leqq |x| \leqq b$, and $b \leqq |x|$, respectively. Table 1 shows the result of conformal transformation with the sign convention $\sqrt{(\pm 1)^2} = \pm 1$ and $\sqrt{-1} = -j$. This mapping is illustrated in Fig. 2 with

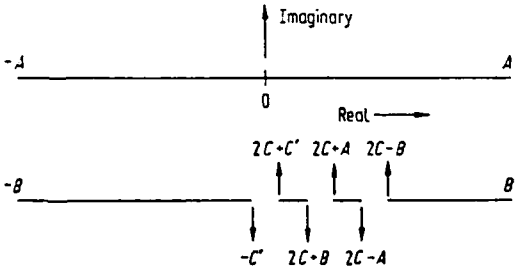

Fig. 2. Two dimensional geometry for the parallel plate transmission line obtained from the geometry of the coplanar waveguide under an elliptical integral transformation.

Table 1. The result of conformal transformation using eqs. (1) and (2) to convert the geometry of coplanar waveguide to the geometry of parallelplate transmission line.

x	$-c'$	$-b$	$-a$	o	a	b
$z(x)$	$-F\left(\alpha, \arcsin\frac{b}{c'}\right)$ $-jF(\frac{\pi}{2}-\alpha, \frac{\pi}{2})$	$-F(\alpha, \frac{\pi}{2})$ $-jF(\frac{\pi}{2}-\alpha, \frac{\pi}{2})$	$-F(\alpha, \frac{\pi}{2})$	o	$F(\alpha, \frac{\pi}{2})$	$F(\alpha, \frac{\pi}{2})$ $-jF(\frac{\pi}{2}-\alpha, \frac{\pi}{2})$

x	$2c-b$	$2c-a$	$2c+a$	$2c+b$	$2c+c'$
$z(x)$	$F\left(\alpha, \arcsin\frac{b}{2c-b}\right)$ $-jF(\frac{\pi}{2}-\alpha, \frac{\pi}{2})$	$F\left(\alpha, \arcsin\frac{b}{2c-a}\right)$ $-jF(\frac{\pi}{2}-\alpha, \frac{\pi}{2})$	$F\left(\alpha, \arcsin\frac{b}{2c+a}\right)$ $-jF(\frac{\pi}{2}-\alpha, \frac{\pi}{2})$	$F\left(\alpha, \arcsin\frac{b}{2c+b}\right)$ $-jF(\frac{\pi}{2}-\alpha, \frac{\pi}{2})$	$F\left(\alpha, \arcsin\frac{b}{2c+c'}\right)$ $-jF(\frac{\pi}{2}-\alpha, \frac{\pi}{2})$

the points $-C'$, $-B$, $-A$, O, A, B, $2C-B$, $2C-A$, $2C+A$, $2C+B$, and $2C+C'$ originating from the integration limits $x=-c'$, $-b$, $-a$, o, a, b, $2c-b$, $2c-a$, $2c+a$, $2c+b$, and $2c+c'$, respectively. The signal conductor with $|x| \leqq a$ in Fig. 1 is mapped to the upper plate in Fig. 2, while the other conductor with $b \leqq |x|$ becomes the lower plate. The second CPW signal conductor located at $(c-a) \leqq |x| \leqq (2c+a)$ is transformed into:

$$\Delta z = F\left(\alpha, \arcsin\frac{b}{2c-a}\right) - F\left(\alpha, \arcsin\frac{b}{2c+a}\right). \quad (4)$$

The metal strip between $2C+A$ and $2C-A$ in Fig. 2 represents the width Δz in eq. (4). The coupling capacitance c between the two CPW signal conductors is estimated from Fig. 2 as a parallel plate capacitance with width Δz, separation $F(\frac{\pi}{2}-\alpha, \frac{\pi}{2})$, and length l as

$$\Delta c\, l = 1{,}5\,(\varepsilon_r+1)\,\varepsilon_0\, l \cdot \frac{F\left(\alpha, \arcsin\frac{b}{2c-a}\right) - F\left(\alpha, \arcsin\frac{b}{2c+a}\right)}{F(\frac{\pi}{2}-\alpha, \frac{\pi}{2})}. \quad (5)$$

Electric field lines originate from the signal conductor 1 and terminate at the signal conductor 2 by way of paths through the underlying substrate and through free space in the region above the CPW plane. These two capacitances in parallel are taken into account by the dielectric constant $(\varepsilon_r+1)\,\varepsilon_0$ in eq. (5), which is equivalent to $2(\varepsilon_r+1)\,\varepsilon_0/2$ with $(\varepsilon_r+1)\,\varepsilon_0/2$ being the effective dielectric constant and 2 representing two capacitances in parallel. The factor 1.5 in this expression is an approximate correction for end effects at the edges of signal conductor 2. We have assumed here that half of the field lines over the gaps adjacent to signal conductor 2 terminate on signal conductor 2 and the remaining half terminate on the ground plane. The value of the correction factor applies in particular to this case with $a=3$ mm and $b=6$ mm, but may be readily modified to suit other CPW geometries.

A simple circuit model for capacitive crosstalk between two CPWs is shown in Fig. 3. Here the coupling

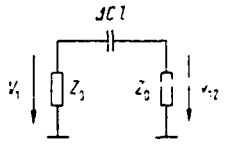

Fig. 3. Circuit model for crosstalk due to capacitive coupling between two closely-spaced coplanar waveguides.

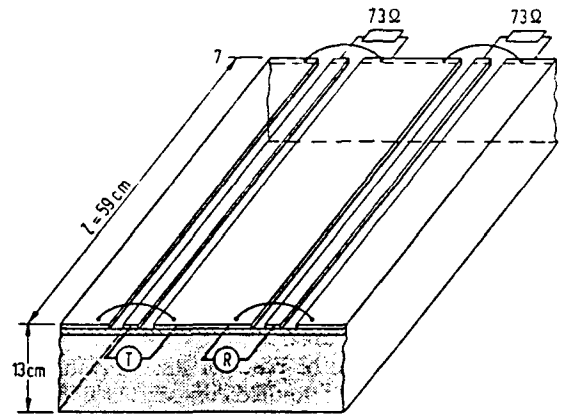

Fig. 4. Crosstalk measurements of two terminated coplanar waveguides with all ground conductors connected together. Here T and R represent signal transmitter and receiver, respectively.

capacitance $\Delta c\, l$ between CPW signal conductors is treated as a lumped element coupling two terminated transmission lines with characteristic impedance Z_0 as shown in Fig. 4 in our crosstalk experiments. The validity of treating $\Delta c\, l$ as a lumped element will be discussed later. According to this circuit model, a sinusoidal signal voltage of frequency f and amplitude V_1 at the input of CPW 1 will generate a crosstalk voltage V_{12} given by

$$j\,2\pi f\,\Delta c\, l\,(V_{12}-V_1)\,Z_0 = V_{12},$$

and the crosstalk between the two CPWs is obtained as

$$T = 10\lg\left|\frac{V_{12}}{V_1}\right|^2 = 10\lg\frac{4\pi^2 f^2 \Delta c^2 l^2 Z_0^2}{1+4\pi^2 f^2 \Delta c^2 l^2 Z_0^2}, \quad (6)$$

where Z_0 may be obtained from Wen's quasi-static calculation [2] of the characteristic impedance of a single isolated CPW:

$$Z_0 = \frac{30\pi}{\sqrt{\frac{(\varepsilon_r+1)}{2}}} \frac{F\left(\frac{\pi}{2}-\alpha, \frac{\pi}{2}\right)}{F\left(\alpha, \frac{\pi}{2}\right)}. \quad (7)$$

The same characteristic impedance Z_0 can also be obtained by dividing the phase velocity $\sqrt{2/\mu_0 \varepsilon_0 (\varepsilon_r+1)}$ with the parallel plate capacitance length derived from Fig. 2.

3. Experiment

Comparison of this model with experiment was achieved by fabricating two up-scaled structures in copper clad epoxy-glass material. A slab of marble ($\varepsilon_r = 6.14$) approximately 13 cm thick simulated the dielectric substrate. Up-scaled dimensions of the coplanar waveguides in Fig. 4 were $2a = 6$ mm, $2b = 12$ mm and a total length $l = 59$ cm. The spacing $2c$ between CPWs was varied from 30 cm to 5 cm by trimming the width of the common ground-plane conductor of each of the CPW structures and rejoining the two with solder to form a single intervening ground plane. The outer ground conductor width is $c' - b = 15$ cm. As shown in Fig. 4, both coplanar waveguides were terminated in 73 Ω which was measured with the aid of a vector impedance bridge. All ground conductors are connected together. Crosstalk between the coplanar waveguides was then measured by increasing the amplitude of a sinusoidal signal applied to CPW 1 until a predetermined signal amplitude was detected in CPW 2. A communication receiver with a fixed gain of 95 dB and a passband of 100 Hz was used to detect the crosstalk signal. The experimental results are shown in Fig. 5 as dotted curves for various CPW separations.

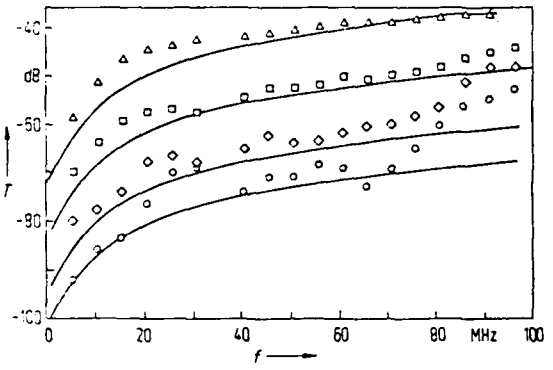

Fig. 5. Crosstalk measured between two 59 cm CPWs vs. operating frequency from 5 MHz to 100 MHz. Here ▵, □, ◇, and ○ are experimental data points for separation $2c = 5$ cm, 10 cm, 20 cm, and 30 cm, respectively. The corresponding theoretical predictions are shown as solid lines. If lateral dimensions are scaled down by a common factor of 100, the crosstalk will be the same for operating frequency 100 times as large (0.5 GHz to 10 GHz).

Assuming an infinitely thick substrate with $\varepsilon_r = 6.14$ (calcite), the characteristic impedance calculated from eq. (7) is $Z_0 = 64\,\Omega$. For CPWs of length $l = 59$ cm in Fig. 4 the coupling capacitances $\Delta c\, l$ calculated from eq. (5) are 10.53 fF, 24.75 fF, 99.35 fF and 400.4 fF with CPW separations $2c = 30$ cm, 20 cm, 10 cm, and 5 cm, respectively. With $Z_0 = 64\,\Omega$ and these coupling capacitances $\Delta c\, l$, Fig. 5 also shows the calculated crosstalks as a function of frequency obtained from eq. (6).

By using much larger CPW structures in these measurements than one might expect to use in real circuit applications, we reduced the relative errors due to stray coupling between feed lines and direct coupling of the signal source and the detector.

4. Discussion and Conclusion

Since the lower plate consists of four disconnected pieces of conductor, the upper plate in Fig. 2 has more metallic area as compared with the lower plate. The relative differences in area are calculated to be 3% for a separation $2c = 5$ cm and 1.6% for $2c = 30$ cm. Thus, the CPW ground conductor in our experiment can be considered as infinitely extended. This is to be expected for two CPWs with large separation, i.e., $2c \gg a$ and $2c \gg b$, because electric fields originated from the signal conductor of CPW 1 find ample ground conductors for their termination.

The substrate thickness is 13 cm which is much larger than the slot width $b - a = 3$ mm. Thus the substrate is practically infinite in thickness [4]. With infinite ground conductors and infinite substrate thickness, eq. (7) predicts the characteristic impedance $Z_0 = 64\,\Omega$ for the substrate relative dielectric constant $\varepsilon_r = 6.14$. This is in contrast with the measured value 73 Ω. The difference may be due to the presence of an air gap between the calcite substrate and the manufactured CPWs on the epoxy glass circuit board. Since the air gap and epoxy glass with $\varepsilon_r = 3.65$ are so close to both signal and ground conductors, they reduce the CPW capacitance per unit and increase the characteristic impedance (from 64 Ω to 73 Ω) as can be expected from eq. (7).

The presence of the air gap and the epoxy glass does affect the predicted value for characteristic impedance. However, it does not change our prediction of the crosstalk based on eqs. (5) and (6). A CPW characteristic impedance is determined mainly by the local electric field distribution adjacent to CPW signal conductor, while the crosstalk due to capacitive coupling between two CPWs with $2c \gg (b - a)$ is determined by the electric field distribution far away from the signal conductor. This latter electric field will pass through the thick (13 cm) substrate. Consequently, the presence of a thin air gap has little effect on crosstalk and the thick calcite substrate is considered as the only substrate in the prediction of crosstalk in eq. (6).

The coupling capacitance $\Delta c\, l$ is represented as a lumped circuit element in Fig. 3 and in eq. (6) for crosstalk prediction. It is a valid representation at low frequency, when the CPW length ($l = 59$ cm) is much

less than the operating signal wavelength. We have experimentally found that $l = 59$ cm was about a quarter wavelength for a 69 MHz signal. Ideally, a distributed capacitive-coupling is needed for operating frequency larger than 69/2 MHz. As shown in Fig. 4, the crosstalk measurements were performed with a transmitter and a receiver at one end of the two CPWs, and two 73 Ω resistors terminated the other end. The traveling wave on CPW 1 from the transmitter will induce traveling waves in both forward and backward directions over the CPW 2 [5]. Only the backward traveling wave on CPW 2 was detected and the forward traveling wave is terminated. The backward traveling waves induced along the whole length (~ 59 cm) of CPW 2 will have different propagating phases at the receiver. Phasor summation of these traveling waves with various phases will result in less crosstalk than eq. (6) at high frequency. This in turn causes the measured crosstalk vs. frequency to be flatter than expected, as can be seen from Fig. 5.

The numerical analysis of crosstalk is made for the two CPWs with a slot width $(b - a)$ equal to half the signal conductor width a (i.e., $(b - a) = a$). If the slot width $(b - a)$ is less than a, then electric fields will be more tightly confined. Consequently, the crosstalk will be less.

The static capacitive coupling model for crosstalk between two CPWs is a good model at low frequency and reasonably close separation (see Fig. 5). As the frequency increases and CPW separation becomes large, we may have to consider the effect of magnetic coupling, which is neglected in this simplified model. The magnetic field coupling has been known to be long ranged [6] and may be responsible for the departure between analytical and experimental results for $2c = 20$ cm and 30 cm in Fig. 5.

The coupling capacitance in eq. (5) and the CPW characteristic impedance in eq. (7) do not depend on the absolute CPW dimensions, of a, b, c, and c'. They depend only on the relative dimensions of a, c, and c' with respect to b. If all dimensions of the CPW in Fig. 4 are scaled down by a factor of 100, then the coupling capacitance per unit length Δc and the CPW characteristic impedance Z_0 in eq. (7) remain the same. However, the total coupling capacitance $\Delta c l$ will be 100 times smaller and, thus the operating frequency f has to increase 100 times (in eq. (6)) to maintain the same crosstalk. Consequently, Fig. 5 is still valid for 100 times down scaled version (with $l = 5.9$ mm) of the CPW in Fig. 4, provided the horizontal axis is increased by a factor of 100 with the unit of 0.1 GHz rather than MHz.

In conclusion, we have calculated the capacitive crosstalk between two coplanar waveguides by mapping of two adjacent CPWs into a parallel geometry using elliptical integral transformations. Reasonably good agreement between the calculated crosstalk and the measured crosstalk in the range of -40 dB to -100 dB was achieved on two up-scaled CPWs of various separations. The difference between theory and experiment is attributed to long ranged magnetic coupling not included in our model and difficulty in accurately measuring the crosstalk as low as -100 dB. Under the process of scaling, both characteristic impedance Z_0 and coupling capacitance per unit length Δc are unchanged. However, the total coupling capacitance $\Delta c l$ and the crosstalk at a given frequency are directly scaled with the CPW length.

This work has been supported by Defense Advanced Research Projects Agency (J. Neff). Technical discussions with and encouragements from R. E. Reedy and D. J. Albares are appreciated.

(Received April 2, 1988.)

Dr. Ching Ten Chang
Department of Electrical and Computer Engineering
San Diego State University
San Diego, CA 92182-0190, USA

Dr. Graham A. Garcia
Naval Ocean Systems Center
San Diego, CA 92152-5000, USA

References

[1] Purcell, R. A.: Design considerations for monolithic microwave circuits. IEEE Trans. MTT-29 (1981), 513–534.
[2] Wen, C. P.: Coplanar waveguide: A surface strip transmission line suitable for nonreciprocal gyromagnetic device applications. IEEE Trans. MTT-17 (1969), 1087–1090.
[3] Jahnke, E.; Emde, F.: Tables of functions. 4th ed. New York: Dover Publ., 1945, 62–65.
[4] Davis, M. E.; Williams, E. W.; Celestini, A. C.: Finite-boundary corrections to the coplanar waveguide analysis. IEEE Trans. MTT-21 (1973), 594–596.
[5] Balakrishnan, R. V.: Cut bus reflections, crosstalk with a trapezoid tranceiver. EDN (1983) 151–156.
[6] Yuan, H. T.; Lin, Y. T.; Chang, S. Y.: Properties of interconnection on silicon, sapphire, and semi-insulating Gallium Arsenide substrates. IEEE Trans. ED-29 (1982), 639–644.